Processing of Chemical Sensor Arrays With a Biologically Inspired Model of Olfactory Coding

Baranidharan Raman, *Member, IEEE*, Ping A. Sun, Agustin Gutierrez-Galvez, and
Ricardo Gutierrez-Osuna, *Member, IEEE*

Abstract—This paper presents a computational model for chemical sensor arrays inspired by the first two stages in the olfactory pathway: distributed coding with olfactory receptor neurons and chemotopic convergence onto glomerular units. We propose a monotonic concentration-response model that maps conventional sensor-array inputs into a distributed activation pattern across a large population of neuroreceptors. Projection onto glomerular units in the olfactory bulb is then simulated with a self-organizing model of chemotopic convergence. The pattern recognition performance of the model is characterized using a database of odor patterns from an array of temperature modulated chemical sensors. The chemotopic code achieved by the proposed model is shown to improve the signal-to-noise ratio available at the sensor inputs while being consistent with results from neurobiology.

Index Terms—Chemical sensor arrays, machine olfaction, olfactory bulb, olfactory receptors.

NOMENCLATURE

EC_{50}	Effective concentration at which the neuron shows half-saturation.
GL	Glomerulus.
GR	Granule.
K_i^L	Affinity of ORN i to ligand L.
L	Ligand.
LOT	Lateral olfactory tract.
MOS	Metal oxide sensor.
M/T	Mitral/tufted cells.
NLA	Normalized log affinity.
OB	Olfactory bulb.
ORN	Olfactory receptor neuron.
P	Pyramidal cells.
PC	Piriform cortex.
PCA	Principal component analysis.
PG	Periglomerular cells.
R_i^L	Response of ORN i to ligand L.
RAD	Receptor affinity distribution.
SBMO	Sensor-based machine olfaction.
SOM	Self-organized map.

I. INTRODUCTION

MOST current approaches for processing data from chemical sensor arrays are the direct application of statistical, chemometrics, and neural pattern recognition techniques [1]. However, biology has always served as an abundant source of inspiration in the design of complex engineering systems. A number of parallels between biological and artificial olfaction are well known to the SBMO community. Two of these parallels are at the core of SMBO, as stated in the seminal work of Persaud and Dodd [2]. First, biology relies on a population of ORNs that are broadly tuned to odorants. In turn, SBMO employs chemical sensor arrays with highly overlapping selectivities. Second, neural circuitry downstream the olfactory epithelium improves the signal-to-noise ratio and the specificity of the initial receptor code, enabling wider odor detection ranges than those of individual receptors. Pattern recognition of chemical sensor signals performs similar functions through preprocessing, dimensionality reduction, and classification/regression algorithms [3]. Unfortunately, ORNs and current chemical sensors detect fundamentally different molecular properties of a volatile compound. For this reason, correlation between chemical sensor patterns and the perceived properties of an odorant, arguably the ultimate role of machine olfaction, have been moderately successful to date [4].

Leaving aside the daunting task of organoleptic prediction, which will necessitate the development of sensing materials attuned to the molecular determinants of odors, a number of olfactory processes are worthy of study for potential application in machine olfaction. These include hyperacuity through sensory integration [5], novelty detection through habituation [6], orthogonalization of sensor patterns through lateral inhibition [7], encoding of odor intensity in interspike intervals [8], concentration-invariant recognition of odors [9], [10], identification against background, segmentation of odor mixtures [11], [12], and perceptual grouping of odors [13]. Moreover, SBMO may serve as a valuable platform for testing olfactory coding and signal processing hypotheses from neurobiology. This modern view of neuromorphic systems [14] reverses the traditional roles of engineering and biology, since the objective becomes using
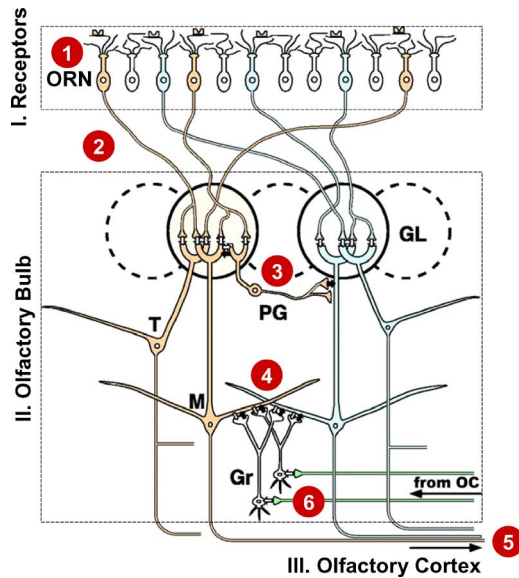
Fig. 1. Different anatomical stages and signal-processing primitives in the olfactory pathway: 1) combinatorial coding, 2) chemotopic convergence, 3) logarithmic compression, 4) contrast enhancement, 5) storage and association of odor memories, and 6) bulbar modulation through cortical feedback (adapted with permission from [17]. (Color version available online at http://ieeexplore.ieee.org.)

an engineering model to validate biological hypotheses rather than designing engineering solutions inspired by biology.

The long-term goal of our research is to develop alternative algorithms for chemical sensor arrays based on known signal-processing principles of the olfactory system. In this paper we present a model of two key elements in the early stages of the olfactory pathway: combinatorial coding with ORNs and chemotopic convergence onto GLs. We first propose a concentration-response model that performs a nonlinear mapping of chemical sensor array data onto a population of simulated ORNs. We then present a self-organizing model of chemotopic convergence capable of generating glomerular activation patterns consistent with those observed in the OB through optical imaging. The complete model is validated using experimental data from an array of metal–oxide gas sensors under temperature-modulation excitation.

II. Signal Processing Primitives in the Olfactory Pathway

The olfactory pathway can be divided into three general stages: 1) olfactory epithelium, where primary reception takes place; 2) olfactory bulb, where an organized olfactory image is formed; and 3) olfactory cortex, where odor associations are stored. These anatomically and functionally distinct relays perform a variety of signal processing tasks, resulting in the sensation that we know as an odor. At the risk of understating the complexity of the olfactory system, six fundamental computational functions can be identified for the purposes of machine olfaction. Illustrated in Fig. 1, these are 1) signal transduction into an ORN combinatorial code, 2) chemotopic convergence of ORN axons onto GL, 3) logarithmic compression through lateral inhibition from PG cells, 4) contrast enhancement through lateral inhibition from GR cells, 5) storage and association

of odor memories, and 6) bulbar modulation through cortical feedback.

The first function is concerned with transduction of the chemical stimulus into an electrical signal. Odorants entering the nostril bind to olfactory receptors and, through secondary messenger mechanisms, transform the chemical stimulus into a neural signal [15]. A complete model of the transduction [16] is beyond the scope of this work; let it suffice that the spiking frequency of an ORN is a monotonically increasing function of the odorant concentration for a given receptor-odorant binding affinity. This dose-response model will be further elaborated in Section IV.

The next three signal processing primitives take place at the OB. The second stage involves massive convergence of ORN axons onto the glomerular layer [17], [18]. As illustrated in Fig. 1, ORNs expressing the same receptor project onto a single or a few target GLs. This form of convergence serves two computational functions. First, massive summation of ORN inputs averages out uncorrelated noise, allowing the system to detect odorants below the detection threshold of individual ORNs [5]. Second, chemotopic organization leads to a more compact odorant representation than that available at the epithelium, providing the means to decouple odor quality from odor intensity. This is the basis for the traditional view of GL as labeled lines or, more recently, as molecular feature (or odotope) detectors [17].

The initial glomerular image is further transformed in the olfactory bulb by means of two distinct lateral inhibitory circuits. The first of these circuits (third primitive in Fig. 1) takes place between proximal GLs through PG cells. As noted by Freeman [19], the interaction through PG cells may serve as a "volume control" mechanism, enabling the identification of odorants over several log units of concentration.

The fourth primitive is represented by dendro-dendritic interactions between excitatory M/T and inhibitory GR cells. These self- and lateral inhibitory circuits form the negative feedback loops that are responsible for the observed oscillatory behavior in OB [20]. More importantly, local inhibition introduces time as an additional dimension for odor coding by generating temporal patterning of the spatial code available at the GL layer [21]. The precise role of the granular lateral inhibition circuits is, however, under debate. The first and more traditional view is that lateral inhibition sharpens the molecular tuning range of individual mitral cells with respect to that of their corresponding ORNs [17]. Taken to the extreme, this function reduces to the winner-take-all strategy of competitive learning. A second hypothesis is that lateral inhibition leads to a "global redistribution" of activity such that the bulb-wide representation of an odorant, rather than the individual tuning ranges, becomes specific and concise over time [18]. This neurodynamics view of lateral inhibition is thus heavily related to temporal coding.

The fifth primitive involves the formation of "odor objects" and the subsequent storage in the PC. Pyramidal neurons, the principal cells in the PC, receive sparse, nontopographic, excitatory connections from M/T axons in the OB through the LOT. These projections are both convergent and divergent (many-to-many). This suggests that P cells detect combinations of co-occurring molecular features of the odorant, and therefore function as "coincidence detectors" [13]. The PC is also characterized by sparse,

distributed connections between P cells. These lateral connections have been shown to play an important role in storing odors with minimum interference and pattern completion of degraded stimuli [22]. Together, these two anatomical features of the PC form the basis for the synthetic processing of odors [13].

The sixth primitive involves centrifugal connections from cortex onto GR interneurons in the olfactory bulb. Several computational functions have been associated with these feedback connections, including odor segmentation and habituation [11], hierarchical clustering [23], and chaotic bulbar dynamics [24]. In the next section, we present a brief review of how these various signal-processing primitives have been adapted for processing data from chemical sensor arrays.

III. REVIEW OF NEUROMORPHIC PROCESSING IN CHEMICAL SENSOR ARRAYS

Leveraging a growing body of knowledge from computational neuroscience [25], neuromorphic models of the olfactory system have become a recent subject of attention for the purpose of processing data from chemical sensor arrays. Ratton *et al.* [26] have employed the olfactory model of Ambros–Ingerson *et al.* [23], which simulates the closed-loop interactions between the olfactory bulb and higher cortical areas. The model performs a hierarchical processing of an input stimulus into increasingly finer descriptions by repetitive projection of bulbar activity to (and feedback from) the olfactory cortex. Ratton *et al.* have applied the model to classify data from a microhotplate metal oxide sensor excited with a saw-tooth temperature profile. Sensor data were converted into a binary representation by means of thermometer and Gray coding, which was then used to simulate the spatial activity at the olfactory bulb. Their results show that classical approaches (Gram–Schmidt orthogonalization, fast Fourier transform, and Haar wavelets) yield better classification performance. This result should come as no surprise given that the thermometer and Gray codes are unable to faithfully simulate the spatial activity at the olfactory bulb, where the most critical representation of an odor stimulus is formed.

White *et al.* [27], [28] have employed a spiking neuron model of the peripheral olfactory system to process signals from a fiber-optic sensor array. In their model, the response of each sensor is converted into a pattern of spikes across a population of ORNs, which then projects to a unique mitral cell. Different odors produce unique spatio-temporal activation patterns across mitral cells, which are then discriminated with a delay line neural network (DLNN). Their OB-DLNN model is able to produce a decoupled odor code: odor quality being encoded by the spatial activity across units and odor intensity by the response latency of the units.

Pearce *et al.* [5] have investigated the issue of concentration hyperacuity by means of massive convergence of ORNs onto GL. Modeling spike trains of individual ORNs as Poisson processes, the authors show that an enhancement in sensitivity of $\sqrt{n}$ can be achieved at the GL, where n is the number of convergent ORNs. Experimental results on an array of optical microbeads are presented to validate the theoretical predictions.

Otto *et al.* have employed the KIII model of Freeman *et al.* [29] to process data from FT-IR spectra [30], [31] and chemical sensors [32]. The KIII is a neurodynamics model that faithfully captures the spatio-temporal activity in the olfactory bulb, as observed in electroencephalogram (EEG) recordings. Different dynamical behaviors can be obtained from the model by careful selection of the coupling coefficients in the KII sets, the coupled oscillators that serve as the basic computational element in the system [33]. In [30], the FT-IR spectrum of each analyte was decimated, Hadamard-transformed, and normalized before being used as an input vector into the KIII model. The authors show that the principal components of the mitral cell state-space attractors can be used to discriminate different analytes. Their results, however, indicate that the KIII is unable to match the performance of a regularized discriminant analysis classifier.

Our prior work [6], [34] has investigated the use of habituation for processing odor mixtures with chemical sensor arrays. A statistical pattern recognition model was presented in [34], where habituation is triggered by a global cortical feedback signal, in a manner akin to Li and Hertz [11]. A neuromorphic approach based on the KIII model was proposed in [6], where habituation is simulated by local synaptic depression of mitral channels. Inspired by the role of GL as functional units [35], sensor array patterns are preprocessed with a family of odor selective discriminant functions before being fed to the KIII model. Our results showed that the KIII model is able to recover the majority of the errors, introduced in the sensor-array and discriminant-function stages, by means of its Hebbian pattern-completion capabilities. We have also proposed a model of the early stages in the olfactory pathway to process data from MOS [36], [37]. The model captures two functions: chemotopic convergence of sensory neurons onto the olfactory bulb, and center on–off surround lateral interactions. The sensor array response is grouped in a manner akin to the convergence of ORN axons onto the glomerular layer. This is subsequently fed to a firing rate model [36] (or a spiking model in [37]) of the olfactory bulb network to code odor identity and intensity in a qualitatively similar manner as in the biological olfactory system.

IV. DOSE-RESPONSE MODEL FOR OLFACTORY RECEPTOR NEURONS

The first stage in the olfactory pathway is a large array ($\sim$10–100 million) of sensory neurons, each of which selectively expresses one or a few genes of a large ($\sim$1000) family of receptor proteins [38]. Each receptor is capable of detecting multiple odorants, and each odorant can be detected by multiple receptors, leading to a massively combinatorial olfactory code at the receptor level. It has been shown [39], [40] that this broad tuning of receptors may be an advantageous strategy for sensory systems dealing with a very large detection space. This is certainly the case for the human olfactory system, which has been estimated to discriminate up to 10 000 different odorants [41].

The response of a particular neuron is determined by the extent to which the receptor binds to the odorant (or ligand). Following [42], the binding of one receptor-ligand pair can be modeled as

$$R_i^L = \frac{1}{1 + \frac{1}{\left(K_i^L [L]\right)^m}} \tag{1}$$

where R_i^L is the average instantaneous firing rate of olfactory receptor neuron $i(\text{ORN}_i)$ when exposed to ligand L at concen-
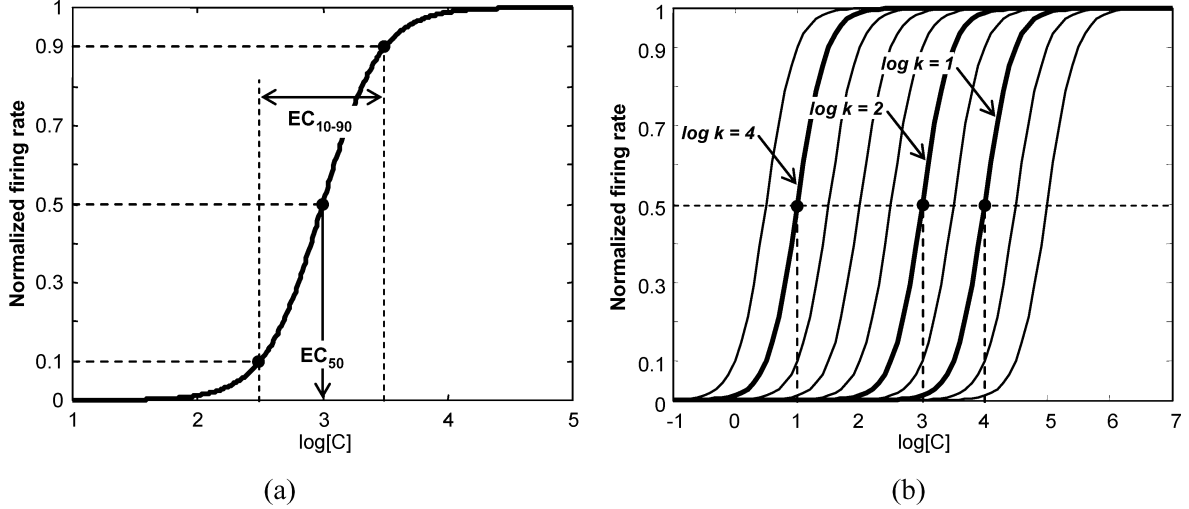
Fig. 2. (a) Concentration-response curve for one ORN. (b) Range of simulated ORN affinities for a particular analyte.

tration $[L]$, K_i^L is the binding affinity between ORN_i and L, and m is the molecular Hill equivalent. Shown in Fig. 2(a), this equation models a monotonic increase in the ORN firing rate with the log-concentration of odor stimulus. The affinity K_i^L can then be interpreted as the inverse of the effective concentration at 50% (EC_{50}), at which the neuron shows half-saturation, whereas m determines its intensity tuning range EC_{10-90}. The effect of the affinity K_i^L on the dose-response curve is illustrated in Fig. 2(b). Following this model, a particular ORN can then be characterized by a vector of log-affinities towards the different volatile compounds (or molecular features) in a given chemical problem space

$$\log \vec{K}_i = \left[\log k_i^1, \log k_i^2, \ldots, \log k_i^n \right]. \qquad (2)$$

V. CHEMOTOPIC CONVERGENCE MODEL

As discussed earlier in Section II, ORNs converge onto the OB in a chemotopic fashion, whereby ORNs expressing the same receptor type project onto a few neighboring GLs. Based on this property, we now present a self-organizing model of convergence that generates a chemotopic projection from a large population of ORNs onto a two-dimensional lattice of GLs [43]. The model exploits the ORN representation in (2), according to which selectivity and sensitivity can be related to the direction and magnitude of the log-affinity vector $\log \vec{K}_i$, respectively. This interpretation is illustrated in Fig. 3(a) for a simple problem with two analytes and six ORNs. Vectors along the shaded angular region (ORN_1 to ORN_3) have similar selectivity profiles but increasing sensitivities. On the contrary, vectors in the shaded radial region (ORN_2 and ORN_4) have similar sensitivities but different selectivity profiles. The key assumption in our model is that, in order to generate a chemotopic projection, ORNs must converge to GL according to their selectivity rather than their sensitivity. Defining an NLA vector $\log \vec{\tilde{K}}_i$ as

$$\log \vec{\tilde{K}}_i = \frac{\log \vec{K}_i}{\sqrt{\sum_{c=1}^{C} \left(\log K_i^{L_c} \right)^2}} \qquad (3)$$

the chemotopic convergence mechanism can be implemented by performing a clustering of the ORN population in NLA space and associating each cluster center to an individual GL. Since GLs are arranged as a single layer in the olfactory bulb, and given that neighboring GLs tend to respond to similar odors [44], [45], a natural choice to model the ORN-GL convergence is the SOM of Kohonen [46]. The SOM is presented with a population of ORNs, each represented by its coordinates in NLA space. Once the SOM is trained to model this population, each ORN is then assigned to the closest SOM node (a virtual GL) in NLA space to form a convergence map. Finally, the response of each GL is computed as the sum of the activity of all ORNs that converge to it

$$G_j^L = \sum_{i=1}^{N} W_{ij} R_i^L \qquad (4)$$

where R_i^L is the firing rate of ORN_i to ligand L and $W_{ij} = 1$ if ORN_i converges to GL_j and zero otherwise. Note that the NLA space is only used to assign each ORN to an individual GL; the ORN and GL responses in (4) are obtained using the unnormalized log-affinity vector $\log \vec{K}_i = \left[\log k_i^1, \log k_i^2, \ldots, \log k_i^n \right]$ and the dose-response model (1).

A. Emerging Olfactory Code

To illustrate the coding capabilities of the chemotopic convergence model, we first present results on a large olfactory system with 400 000 ORNs and a 20×20 SOM lattice [43], which yields a realistic convergence ratio of 1000:1. The probabilistic distribution of ORN log-affinities $\{\log K_1^L, \log K_2^L, \ldots, \log K_N^L\}$ for analyte L across a repertoire of N receptors is modeled with the RAD of Lancet et al. [47], which states that the probability of a given ORN type is inversely proportional to its affinity K. The RAD is a universal model for ligand-receptor interactions that has been shown to provide theoretical estimates of receptor repertoire size that are consistent with the experimental studies of Buck and Axel [38]. Standard parameter settings of the RAD ($B = 10$,
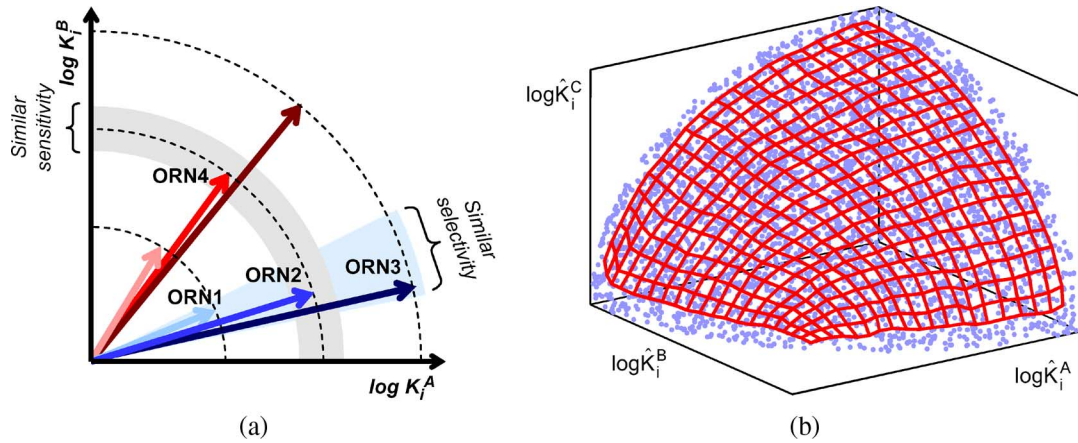
Fig. 3. (a) Interpretation of selectivity and sensitivity from the log-affinity vector. (b) Glomerular SOM (red) and ORN repertoire (cyan) in normalized log-affinity space for a simulated three-analyte chemical space. (Color version available online at http://ieeexplore.ieee.org.)
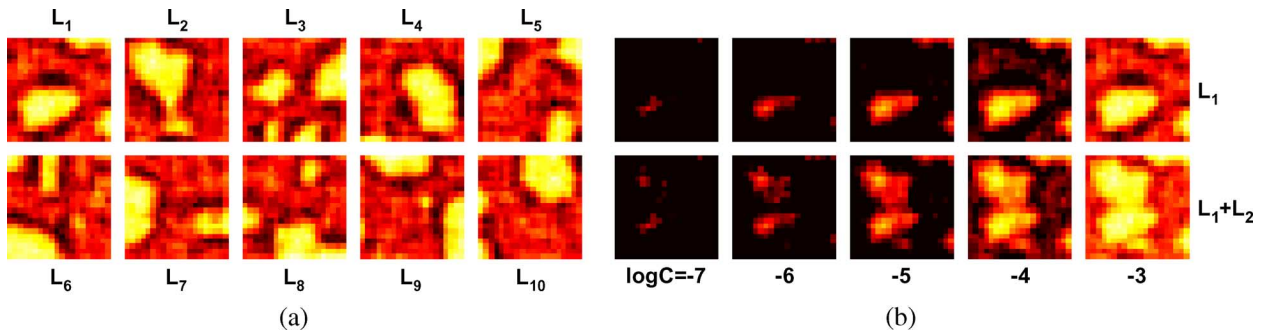

Fig. 4. (a) Glomerular images for ten different ligands at 10^{-3} M. Each ligand produces a unique spatial pattern across the GL layer. (b) Glomerular images for ligand L_1 and the mixture $L_1 + L_2$ at increasing concentrations from 10^{-7} to 10^{-3} M. (Color version available online at http://ieeexplore.ieee.org.)

$S = 8$, and $\alpha = 1.4 Kcal \cdot mol^{-1}$) are used in this paper. In this case, ORN activities are simulated according to (1) since collecting sensor-array patterns for a large number of analytes and concentrations is impractical. Results on experimental data from the sensor array are presented in Section VI.

In order to illustrate the NLA distribution and the ORN-to-GL convergence mapping, the model is first trained on a hypothetical chemical space with only three analytes. The simulation results are shown in Fig. 3(b). Due to the normalization step in (3), the ORN population in NLA space follows a uniform distribution on a unit-radius spherical manifold. In turn, the trained SOM lattice arranges itself to model this NLA distribution, as illustrated by the two-dimensional mesh in Fig. 3(b).

In order to analyze the emerging olfactory code, the model is finally simulated on a larger chemical space with ten analytes. After training, the SOM is exposed to (simulated) concentrations of the analytes ranging from 10^{-7} M to 10^{-3} M, resulting in the 20×20 glomerular images shown in Fig. 4. The glomerular response of the different analytes at a fixed concentration of 10^{-3} M is shown in Fig. 4(a), whereas the glomerular activities at different concentration for analyte L_1 and the mixture L_{1+2} are shown in Fig. 4(b). These results show that each analyte elicits a unique glomerular image with higher activity in those GLs that receive projections from ORNs with high affinity to that analyte. As the concentration of the analyte increases, additional ORNs with lower affinity are recruited, resulting in an increased activation level and a larger spread of the analyte-specific loci. These results are consistent with those from experi-

mental data in neurobiology [45], [48], [49]: spatially local activity, and decoupling of odor identity/concentration.

VI. PROCESSING OF CHEMICAL SENSOR DATA

The sensor array employed in this paper consists of two MOS chemoresistors [50]. These sensors are widely available commercially from several vendors, are fairly stable, and provide good sensitivity for various solvents and combustible gases. However, MOS sensors are known to be poorly selective. Their selectivity is partly determined by the operating temperature, normally set by applying a fixed excitation voltage across a resistive heater built into the device. It has been shown [51] that this thermal dependence can be used to improve the selectivity of the sensor by modulating the heater voltage and capturing the sensor response at multiple temperatures. This excitation principle is commonly referred to as temperature modulation [52]. Two types of temperature-modulation profiles are commonly employed: temperature cycling and temperature transients [53]. In temperature cycling, the sensor is excited with a continuous heater voltage, typically a sinusoidal waveform, to ensure a smooth temperature profile. If the heater waveform is slow enough to allow the sensor to keep up with the set-point temperature, the behavior of the sensor at each temperature may then be thought of as a "pseudosensor" by virtue of the temperature-selectivity dependence. In thermal transients, on the other hand, the sensor is driven by a step or pulse waveform in the heater voltage, and the discriminatory
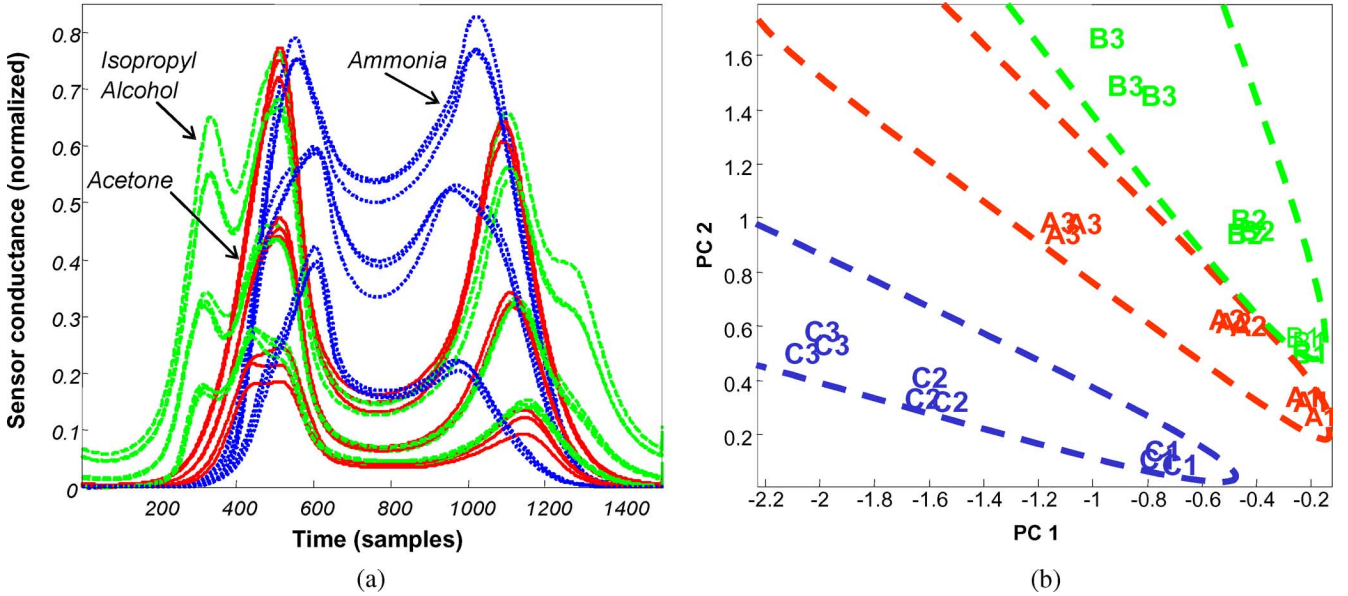
Fig. 5. (a) Temperature modulated response of a TGS2600 sensor to three concentrations three analytes at three concentration. (b) PCA scatter plot of serial dilutions from three analytes. Increasing subindexes (one to three) denote higher concentrations. (Color version available online at http://ieeexplore.ieee.org.)

information is contained in the chemical transient induced by the fast change in temperature.

In this paper, we employ temperature cycling with sinusoidal waveform (0–7 V, $T = 150$ s, 10 Hz sampling frequency). The sensor array was exposed to the static headspace of mixtures from three analytes: acetone (A), isopropyl alcohol (I), and ammonia (M) at three dilution levels in distilled water (the neutral). The lowest dilution of the analytes was 0.3 v/v% for acetone, 1.0 v/v% for isopropyl alcohol, and 33 v/v% for ammonia. These baseline dilutions were chosen so that the average isothermal response (i.e., a constant heater voltage of 5 V) across the two sensors was similar for the three analytes, thus ensuring that they could not be trivially discriminated. Two serial dilutions with a dilution factor of 1/3 were also acquired, resulting in 15 samples per day (four mixtures × three concentrations, plus three neutral samples). The process was repeated on three separate days, for a total of 45 samples. The temperature-modulated response of one of the sensors to the three concentrations of the single analytes is shown in Fig. 5. The sinusoidal heater voltage starts at 0 V at $t = 0$ samples, reaches a maximum of 7 V at $t = 750$ samples, and returns to 0 V at $t = 1500$ sa. Each analyte leads to a unique pattern, defined by the amplitude and location of a maximum in conductance. Two maxima are easily resolved in the case of isopropyl alcohol.

To extract information from the temperature modulated response, each transient was decimated into ten equally spaced measurements per sensor, generating a 20-dimensional odor signal from the sensors. The response to distilled water was subtracted from the response to each analyte in order to make the origin of feature space coincide with the neutral odor. A PCA reduction of this high-dimensional vector, illustrated in Fig. 5(b), shows a unique concentration gradient for each of the three analytes, with increasing separability at higher concentrations (higher subindexes), as could be expected.

A. Mapping Sensor Patterns Onto Firing Rates

To simulate an ORN population with a chemical sensor array, a mapping is required from the feature space in Fig. 5(a) onto firing rates according to the monotonic dose-response model in (1). For this purpose, we propose a receptor model that transforms the n-dimensional sensor response $\overrightarrow{S^A} = [S_1^A, S_2^A, \ldots, S_n^A]$, where S_j^A is the response of sensor j to odor A, onto an m-dimensional response $\overrightarrow{R^A} = [R_1^A, R_2^A, \ldots, R_m^A]$ across a population of m $(m \gg n)$ ORNs. The selectivity of each simulated ORN is given by an n-dimensional unit vector $\overrightarrow{V_i} = [V_1, V_2, \ldots, V_n]$ defined in feature space, as illustrated in Fig. 6(a). The response of receptor i to odor A is then given by

$$R_i^A = \sigma \left(|S^A| \cdot \cos \left(\theta_{V_i, S^A} \right)^p \right) \qquad (5)$$

where $|S^A|$ is the length of the odor vector, which captures concentration information, θ_{V_i, S^A} is the angle between the vectors $\overrightarrow{V_i}$ and $\overrightarrow{S^A}$, which is related to the identity of the odor, p defines the receptive field width of this receptor [refer to Fig. 6(b)], and $\sigma(\cdot)$ is a logistic function that models saturation. The cosine weighting of the form shown in (5) is common in the primary motor neurons used to code movement directions [54] and has been suggested to be a primary requirement for performing vector computations on sensory inputs [55].

Let us illustrate this mapping with an example. Consider a synthetic problem with two gas sensors (1 and 2) and three receptors (A, B, and C). The surface plot in Fig. 7 shows the response of each simulated ORN to all possible combinations of sensor 1 and sensor 2 responses. Receptor A is selective to odors that produce high response in sensor 2 and low response in sensor 1. Receptors B and C, which have similar selectivity, respond maximally to odors that generate high response in sensor
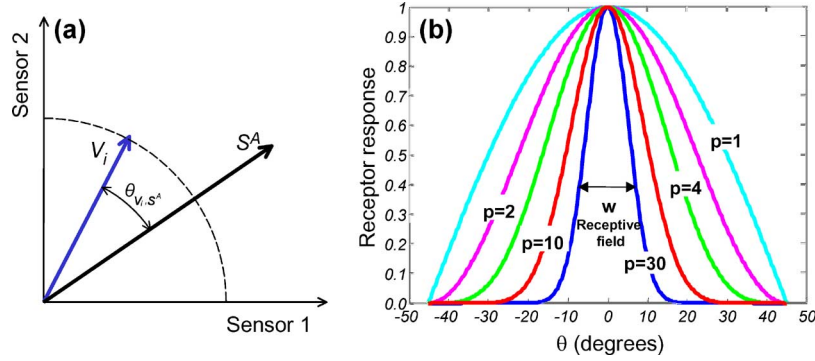
Fig. 6. (a) Illustration of the receptor model: The selectivity of receptor neuron i is defined by the unit vector V_i in a two-dimensional sensor space. The response of this receptor to odor A depends on the angle θ_{V_i, S^A} between V_i and the sensor response to the odor $S^A = [S_1, S_2]$. (b) Effect of parameter p on the cosine weights: large value of p corresponds to narrow receptive field widths and small p values corresponds to broad receptive field widths. (Color version available online at http://ieeexplore.ieee.org.)
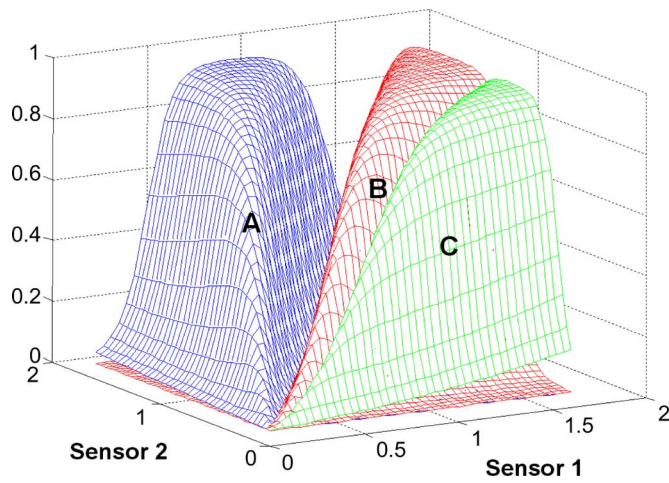

Fig. 7. Illustration of the receptor mapping: Three receptors and their receptive field defined in a synthetic two dimensional sensor space. (Color version available online at http://ieeexplore.ieee.org.)

1 but low response in sensor 2. Furthermore, the response of the receptors increases with an increase in concentration (represented by an increase in the amplitude of the sensor response) and saturates. By sampling the sensor space with a population of such simulated receptors, a high-dimensional odor signal can be obtained that preserves the topology and proximity relationships of the sensor space.

B. Chemotopic Convergence Model

In order to evaluate the proposed dose-response and chemotopic convergence models on experimental data from the sensor array, a smaller olfactory system with 5000 ORNs and a 10 × 10 SOM lattice was used. The sensor response (only one out of three replicates) to each of the three analytes (A, I, M) at their highest concentration was used to train the system. Since uniformly sampling the 20-dimensional space with 5000 ORNs would lead to a very sparse representation, the simulated ORNs were aligned in the direction of the three training odor vectors with the addition of uniformly distributed noise to each dimension ($\pm 25\%$ of the maximum value) to prevent overfitting. The SOM was then trained using a fixed learning rate and a decaying neighborhood width (refer to [56; p. 450] for equations). Fig. 8

shows the simulated glomerular images (SOM activity) for the three analytes (A, I, M) at three dilution levels. Lighter areas in the SOMs identify nodes that show high activity to the input odor, whereas darker regions correspond to nodes that are not active. These GL images present a simpler structure than that in Fig. 4, primarily due to the fact that only three analytes are used and, therefore, the SOM needs to learn only three odor-specific loci. Besides this quantitative difference, the glomerular SOM is capable of decoupling odor quality from odor intensity, quality being encoded by the spatial pattern across glomeruli, and intensity being captured by the amplitude and spread of this pattern. An interesting observation to be made at this point is that the locus of activity for a given odor corresponds to those SOM nodes that receive projections from the temperature features of maximum gain to that odor.

Fig. 9 shows the response of the system to a mixture of acetone and isopropyl alcohol at three different concentrations, which resembles the sum of the activation produced by any of its individual components. This form of additive effect, where the perceived strength of the mixture is equal to the sum of the perceived strengths of its components, is known to occur during perceptual processing of odor mixtures [57].

Apart from the qualitative similarity with the processing of odors in the biological olfactory system, what are the pattern recognition advantages of the proposed model? To answer this question, we employ a measure of class separability derived from Fisher's linear discriminant analysis [58]

$$J = \frac{tr(S_B)}{tr(S_W)} \tag{6}$$

where S_W and S_B are the within-class and between-class scatter matrices, respectively, defined as follows:

$$S_W = \sum_{q=1}^{Q} \sum_{x \in \omega_q} (x - \mu_q)(x - \mu_q)^T \tag{7}$$

$$S_B = \sum_{q=1}^{Q} (\mu_q - \mu)(\mu_q - \mu)^T \tag{8}$$

$$\mu_q = \frac{1}{n_q} \sum_{x \in \omega_q} x \quad \text{and} \quad \mu = \frac{1}{n} \sum_{\forall x} x \tag{9}$$
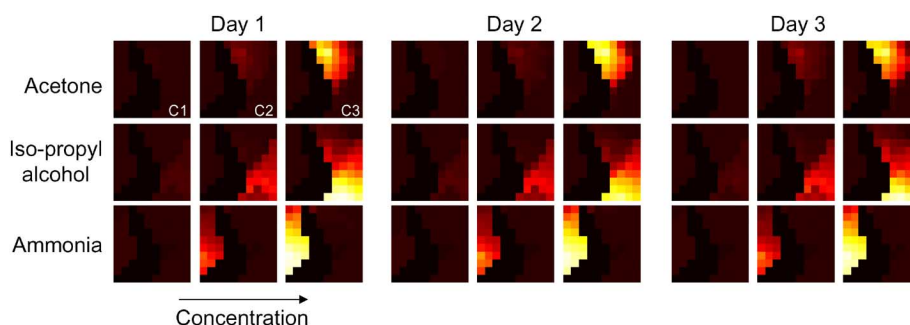
Fig. 8. Glomerular images of the three analytes generated using an experimental database of temperature-modulated MOS sensors exposed to acetone, isopropyl alcohol, and ammonia at three different concentrations levels [refer to Fig. 5(a)]. Lighter areas in the SOMs identify nodes that show high activity to the input odor, whereas darker regions correspond to nodes that are not active. Three replicates per analyte and concentration are shown in the figure to illustrate the repeatability of the spatial patterns. A population of 5000 sharply tuned receptor neurons ($p = 30$) and a 10×10 SOM lattice was used to generate these spatial maps. (Color version available online at http://ieeexplore.ieee.org.)
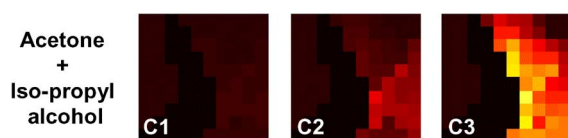

Fig. 9. Glomerular images generated from the sensor array response to a mixture of acetone and isopropyl alcohol at three concentrations. Lighter areas in the SOMs identify nodes that show high activity to the input odor, whereas darker regions correspond to nodes that are not active. (Color version available online at http://ieeexplore.ieee.org.)
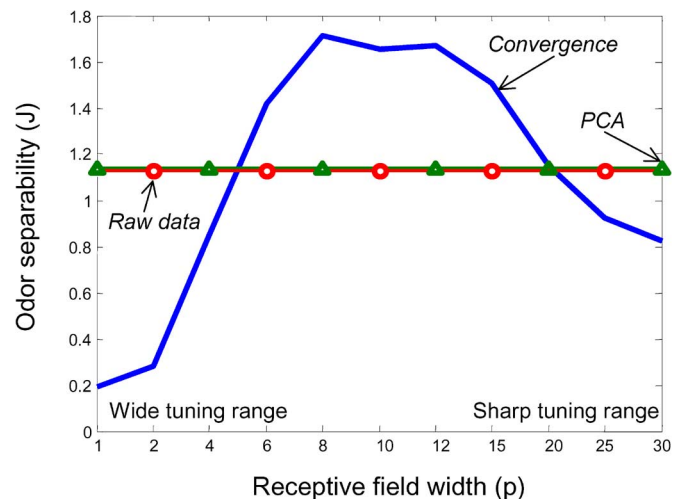

Fig. 10. Comparison of pattern separability using (a) raw sensor data (circles), (b) PCA (triangles), and (c) convergence: maximum separability is achieved in the region $p = 8$ to $p = 12$. (Color version available online at http://ieeexplore.ieee.org.)

where x is a feature vector, Q is the number of odor classes, μ_q and n_q are the mean vector and number of examples for odor q, respectively, n is the total number of examples in the data set, and μ is the mean vector of the entire distribution. Being the ratio of the spread between classes relative to the spread within each class, the measure J increases monotonically as classes become increasingly more separable.

Fig. 10 shows the separability between the three analytes (all concentrations included) when computed from raw sensor data (20 dimensions), principal components (first two PCs), and following convergence mapping. Odor separability is constant for

raw data and PCA since these representations are not a function of the receptive field width. Maximum separability is achieved using convergence mapping with receptor neurons whose receptive field width is neither too broad nor too narrow ($p = 8$ to $p = 12$). This is in agreement with theoretical work on biological and artificial chemical sensors, which indicates that maximum mutual information between the sensor response and the set of odors to be identified is obtained by using an array of receptors/sensors that are tuned to 25–35% of the entire stimuli set [39]. Furthermore, our results show that convergence (for $6 \leq p \leq 15$) leads to an increase in odor separability when compared with the raw signals or the PCA projection. This improvement in signal-to-noise-ratio is a direct result of the supervised nature of the convergence mapping, which leads to more orthogonal patterns than those available at the input.

VII. DISCUSSION

This paper has presented a computational model for chemical sensor arrays inspired by the first two stages in the olfactory pathway: Population coding with broadly tuned olfactory receptor neurons and chemotopic convergence onto glomerular units. Each receptor is modeled by a vector of log-affinities towards the different analytes in chemical space. Combined with a monotonic concentration-response curve, this model can be used to define a nonlinear mapping from chemical sensor-array patterns onto firing rates. The rationale behind our mappings from sensor data onto a high-dimensional ORN population is that, in order to exploit the strategies employed by the olfactory system, our model must operate with a similar representation to that available in the epithelium (i.e., combinatorial and high-dimensional).

The first of such biologically inspired strategies is the convergence mapping presented in this manuscript. Olfactory receptor neurons are assumed to project onto the olfactory bulb according to their selectivity profile, defined as a normalized vector of affinities towards different volatile compounds. A Kohonen SOM is used to cluster olfactory receptor neurons in a topology-preserving fashion, leading to a two-dimensional spatial patterning of activity that are consistent with results observed in the biological olfactory bulb through optical imaging. Note that the SOM is used to cluster sensor features that have similar affinities (similar class information) rather than to cluster

similar examples, as is conventionally done in pattern recognition: clustering is done in the "affinity space" rather than in the conventional "feature space." It is this novelty in training the SOM that leads to spatial odor maps that are qualitatively similar to those found in biology [45], [48], [49]. The chemotopic convergent projection produces unique spatial patterns for each analyte, effectively decoupling odor quality from odor intensity, which cannot be accomplished at the receptor level. This emerging code is analyzed on a large model consisting of 400 000 receptors and 400 glomeruli using simulated data, and also on a smaller model with 5000 receptors and 100 glomeruli using actual data from a gas sensor array.

Our results on sensor data show that maximum separability is achieved with a receptive field that is neither too broad nor too narrow. Our model has employed a homogeneous receptor population. However, theoretical predictions by Alkasab *et al.* [39] have shown that maximum mutual information is achieved with a heterogeneous population of receptors/sensors. It is therefore possible that improved pattern separability may be obtained by employing a nonuniform distribution of receptor field widths (parameter p in our model). An additional but related direction for future work is to study the generalization properties of the model when exposed to unseen odors (or mixtures of learned odors). Clearly, there exists a tradeoff between selectivity and generality. With a receptive field tuned to the odors in the training set (as has been done in this paper), the system may be unable to respond to new odors if these lie on undersampled regions in feature space. A heterogeneous distribution of receptor field widths may again be the solution to balance both goals.

The overall objective of our research is to develop a pattern recognition architecture that incorporates all of the processing stages identified in Section II. To this effect, we intend to integrate the proposed chemotopic convergence mechanism with models of periglomerular volume control [59], granule contrast enhancement [36], [37], and bulbar-cortical interactions [60] that are being developed by our group.

REFERENCES

[1] R. Gutierrez-Osuna, "Pattern analysis for machine olfaction: A review," *IEEE Sensors J.*, vol. 2, no. 3, pp. 189–202, Apr. 2002.

[2] K. C. Persaud and G. H. Dodd, "Analysis of discrimination mechanisms of the mammalian olfactory system using a model nose," *Nature*, vol. 299, pp. 352–355, 1982.

[3] T. C. Pearce, "Computational parallels between the biological olfactory pathway and its analogue 'The Electronic Nose': Part II—sensor-based machine olfaction," *BioSyst.*, vol. 41, pp. 69–90, 1997.

[4] M. C. Burl, B. J. Doleman, A. Schaffer, and N. S. Lewis, "Assessing the ability to predict human percepts of odor quality from the detector responses of a conducting polymer composite-based electronic nose," *Sens. Actuators B Chem.*, vol. 72, no. 2, pp. 149–159, 2001.

[5] T. C. Pearce, P. F. M. J. Verschure, J. White, and J. S. Kauer, "Robust stimulus encoding in olfactory processing: hyperacuity and efficient signal transmission," in *Emergent Neural Computation Architectures Based on Neuroscience*, S. Wermter, J. Austin, and D. Willshaw, Eds. Berlin, Germany: Springer-Verlag, 2001, pp. 461–479.

[6] R. Gutierrez-Osuna and A. Gutierrez-Galvez, "Habituation in the KIII olfactory model with chemical sensor arrays," *IEEE Trans. Neural Netw.*, vol. 40, no. 6, pp. 649–656, Nov. 2003.

[7] G. A. Cecchi, L. Petreanu, A. Alvarez-Buylla, and M. Magnasco, "Unsupervised learning and adaptation in a model of adult neurogenesis," *J. Comput. Neurosci.*, vol. 11, no. 2, pp. 175–182, 2001.

[8] A. G. Lozowski, M. Lysetskiy, and J. M. Zurada, "Signal processing with temporal sequences in olfactory systems," *IEEE Trans. Neural Netw.*, vol. 15, no. 5, Sep. 2004.

[9] A. Backer, "Pattern recognition in locust early olfactory circuits: Priming, gain control and coding issues," Ph.D. dissertation, Dept. Biology, California Inst. Tech., Pasadena, CA, 2002.

[10] P. Cariani, "Temporal codes and computations for sensory representation and scene analysis," *IEEE Trans. Neural Netw.*, vol. 15, no. 5, pp. 1100–1111, Sep. 2004.

[11] Z. Li and J. Hertz, "Odor recognition and segmentation by a model olfactory bulb and cortex," *Network Comput. Neural Syst.*, vol. 11, pp. 83–102, 2000.

[12] D. Wang, J. Buhmann, and C. von der Malsburg, "Pattern segmentation in associative memory," *Neural Comput.*, vol. 2, pp. 94–106, 1990.

[13] D. A. Wilson and R. J. Stevenson, "The fundamental role of memory in olfactory perception," *Trends Neurosci.*, vol. 26, no. 5, pp. 243–247, 2003.

[14] B. Webb, "What does robotics offer animal behaviour?," *Animal Behav.*, vol. 60, pp. 545–558, 2001.

[15] S. Firestein, "How the olfactory system makes sense of scents," *Nature*, vol. 413, pp. 211–218, 2001.

[16] R. Malaka, T. Ragg, and M. Hammer, "A model for chemosensory reception," in *Adv. Neural Inf. Process. Syst.*, G. Tesauro, D. S. Touretzky, and T. K. Leen, Eds. Cambridge, MA: MIT Press, 1995, vol. 7, pp. 61–68.

[17] K. Mori, H. Nagao, and Y. Yoshihara, "The olfactory bulb: Coding and processing of odor molecule information," *Science*, vol. 286, no. 5440, pp. 711–715, 1999.

[18] G. Laurent, "A systems perspective on early olfactory coding," *Science*, vol. 286, no. 5440, pp. 723–728, 1999.

[19] W. Freeman, "Olfactory system: Odorant detection and classification," in *Building Blocks for Intelligent Systems: Brain components as Elements of Intelligent Function*, D. Amit and G. Parisi, Eds. New York: Academic, 1999, vol. III, pt. 2.

[20] I. Segev, "Taming the time in the olfactory bulb," *Nature Neurosci.*, vol. 12, no. 12, pp. 1041–1042, 1999.

[21] G. M. Shepherd and C. A. Greer, "The olfactory bulb," in *The Synaptic Organization of the Brain*, G. M. Shepherd, Ed. Oxford, U.K.: Oxford Univ. Press, 1998, pp. 159–203.

[22] M. A. Wilson and J. M. Bower, "A computer simulation of olfactory cortex with functional implications for storage and retrieval of olfactory information," in *Neural Information Processing Systems*, D. Z. Anderson, Ed. New York: American Inst. of Physics, 1988, pp. 114–126.

[23] J. Ambros-Ingerson, R. Granger, and G. Lynch, "Simulation of paleocortex performs hierarchical clustering," *Science*, vol. 247, pp. 1344–1348, 1990.

[24] Y. Yao and W. J. Freeman, "Model of biological pattern recognition with spatially chaotic dynamics," *Neural Netw.*, vol. 3, pp. 153–170, 1990.

[25] J. L. Davis and H. Eichenbaum, Eds., *Olfaction: A Model System for Computational Neuroscience*. Cambridge, MA: MIT Press, 1991.

[26] L. Ratton, T. Kunt, T. McAvoy, T. Fuja, R. Cavicchi, and S. Semancik, "A comparative study of signal processing techniques for clustering microsensor data (a first step towards an artificial nose)," *Sens. Actuators B Chem.*, vol. 41, no. 1–3, pp. 105–120, 1997.

[27] J. White, T. A. Dickinson, D. R. Walt, and J. S. Kauer, "An olfactory neural network for vapor recognition in an artificial nose," *Biol. Cybern.*, vol. 78, pp. 245–251, 1998.

[28] J. White and J. S. Kauer, "Odor recognition in an artificial nose by spatio-temporal processing using an olfactory neuronal network," *Neurocomput.*, vol. 26–27, pp. 919–924, 1999.

[29] H. J. Chang, W. J. Freeman, and B. C. Burke, "Biologically modeled noise stabilizing neurodynamics for pattern recognition," *Int. J. Bifurcat. Chaos*, vol. 8, no. 2, pp. 321–345, 1998.

[30] S. Quarder, U. Claussnitzer, and M. Otto, "Using singular-value decompositions to classify spatial patterns generated by a nonlinear dynamic model of the olfactory system," *Chemometrics Intell. Lab. Syst.*, vol. 1248, pp. 45–51, 2001.

[31] U. Claussnitzer, S. Quarder, and M. Otto, "Interpretation of analytical patterns from the output of chaotic dynamical memories," *Fresenius J. Anal. Chem.*, vol. 369, pp. 698–703, 2001.

[32] M. Otto, S. Quarder, U. Claußnitzer, and J. Lerchner, "A nonlinear dynamic system for recognizing chemicals based on chemical sensors and optical spectra," in *Proc. World Multiconf. Systems, Cybernetics Informatics*, 2000, vol. X, pp. 413–418.

[33] D. Xu and J. Principe, "Dynamical analysis of neural oscillators in an olfactory cortex model," *IEEE Trans. Neural Netw.*, vol. 15, no. 5, pp. 1053–1062, Sep. 2004.

[34] R. Gutierrez-Osuna and N. U. Powar, "Odor mixtures and chemosensory adaptation in gas sensor arrays," *Int. J. Artif. Intell. Tools*, vol. 12, no. 1, pp. 1–16, 2003.

[35] T. C. Pearce, "Computational parallels between the biological olfactory pathway and its analogue 'The Electronic Nose': Part I—Biological olfaction," *BioSyst.*, vol. 41, pp. 43–67, 1997.

[36] B. Raman, R. Gutierrez-Osuna, A. Gutierrez-Galvez, and A. Perera-Lluna, "Sensor-based machine olfaction with a neurodynamics model of the olfactory bulb," in *Proc. 2004 IEEE/RSJ Int. Conf. Intelligent Robots Systems*, Sendai, Japan, Sep. 28–Oct. 2 2004.

[37] B. Raman and R. Gutierrez-Osuna, "Chemosensory processing in a spiking model of the olfactory bulb: Chemotopic convergence and center surround inhibition," in *NIPS 2004*, Vancouver, BC, Canada, Dec. 13–16, 2004.

[38] L. Buck and R. Axel, "A novel multigene family may encode odorant receptors: A molecular basis for odor recognition," *Cell*, vol. 85, pp. 175–187, 1991.

[39] T. K. Alkasab, J. White, and J. S. Kauer, "A computational system for simulating and analyzing arrays of biological and artificial chemical sensors," *Chem. Sens.*, vol. 27, pp. 261–275, 2002.

[40] K. Zhang and T. J. Sejnowski, "Neuronal tuning: to sharpen or broaden," *Neural Comput.*, vol. 11, pp. 75–84, 1999.

[41] S. S. Schiffman and T. C. Pearce, "Introduction to olfaction: Perception, anatomy, physiology, and molecular biology," in *Handbook of Machine Olfaction: Electronic Nose Technology*, T. C. Pearce, S. S. Schiffman, H. T. Nagle, and J. W. Gardner, Eds. New York: Wiley, 2003.

[42] T. A. Cleland and C. Linster, "Concentration tuning mediated by spare receptor capacity in olfactory sensory neurons," *Neural Comput.*, vol. 11, pp. 1673–1690, 1999.

[43] R. Gutierrez-Osuna, "A self-organizing model of chemotopic convergence for olfactory coding," in *Proc. 2nd Joint EMBS-BMES Conf.*, Houston, TX, Oct. 2002, pp. 23–26.

[44] M. Meister and T. Bonhoeffer, "Tuning and topography in an odor map on the rat olfactory bulb," *J. Neurosci.*, vol. 21, no. 4, pp. 1351–1360, 2001.

[45] B. A. Johnson and M. Leon, "Modular representation of odorants in the glomerular layer of the rat olfactory bulb and the effects of stimulus concentration," *J. Comp. Neurol.*, vol. 422, pp. 496–509, 2000.

[46] T. Kohonen, "Self-organized formation of topologically correct feature maps," *Biol. Cybern.*, vol. 43, pp. 59–69, 1982.

[47] D. Lancet, E. Sadovsky, and E. Seidelmann, "Probability model for molecular recognition in biological receptor repertoires: significance to the olfactory system," *Proc. Nat. Acad. Sci.*, vol. 90, pp. 3715–3719, 1993.

[48] J. Joerges, A. Küttner, C. G. Galizia, and R. Menzel, "Representations of odours and odour mixtures visualized in the honeybee brain," *Nature*, vol. 387, pp. 285–288, 1997.

[49] R. W. Friedrich and S. I. Korsching, "Combinatorial and chemotopic odorant coding in the zebrafish olfactory bulb visualized by optical imaging," *Neuron*, vol. 18, pp. 737–752, 1997.

[50] Figaro Engineering, Inc, Figaro 1996 Osaka, Japan.

[51] W. M. Sears, K. Colbow, and F. Consadori, "Algorithms to improve the selectivity of thermally-cycled tin oxide gas sensors," *Sens. Actuators B*, vol. 19, no. 4, pp. 333–349, 1989.

[52] A. P. Lee and B. J. Reedy, "Temperature modulation in semiconductor gas sensing," *Sens. Actuators B*, vol. 60, pp. 35–42, 1999.

[53] R. Gutierrez-Osuna, A. Gutierrez-Galvez, and N. Powar, "Transient response analysis for temperature modulated chemoresistors," *Sens. Actuators B*, vol. 93, no. 1–3, pp. 57–66, 2003.

[54] A. Georgopoulos, A. B. Schwartz, and R. E. Kettner, "Neuronal population coding of movement direction," *Science*, vol. 233, no. 4771, pp. 1416–1419, 1986.

[55] H. R. Wilson, *Spikes Decision and Actions, Dynamical Foundations of Neuroscience*. Oxford, U.K.: Oxford Univ. Press, 1999.

[56] S. Haykin, *Neural Networks: A Comprehensive Foundation*, 2nd ed. Upper Saddle River, NJ: Prentice-Hall, 1999.

[57] D. G. Laing and A. L. Jinks, "Psychophysical analysis of complex odor mixtures," *Chimia*, vol. 55, pp. 413–420, 2001.

[58] K. Fukanaga, *Statistical Pattern Recognition*, 2nd ed. San Diego, CA: Academic, 1990.

[59] B. Raman and R. Gutierrez-Osuna, "Concentration normalization with a model of gain control in the olfactory bulb," in *Proc. 11th Int. Symp. Olfaction Electronic Nose (ISOEN 2005)*, Barcelona, Spain, Apr. 13–15, 2005.

[60] ——, "Mixture segmentation and background suppression in chemosensor arrays with a model of olfactory bulb-cortex interaction," in *Proc. 2005 IEEE Int. Joint Conf. Neural Networks*, Montreal, PQ, Canada, Jul. 31–Aug. 4 2005, vol. 1, pp. 131–136.

Baranidharan Raman (S'03–M'05) received the B.Eng. degree in computer science (with distinction) from the University of Madras, India, in 2000 and the M.S. and Ph.D. degrees in computer science from Texas A&M University, College Station, in 2003 and 2005, respectively.

He is currently a Postdoctoral Researcher with the Laboratory of Cellular and Synaptic Physiology, National Institutes of Health (NIH) and the Processing Sensing Group, National Institute of Standards and Technology (NIST). His research interests include sensor-based machine olfaction, neural computation, computational neuroscience, intelligent systems, machine learning, neural computation, and robotics.

Ping A. Sun received the B.S. and M.S. degrees in computer engineering from Shandong University of Technology, China, in 1994 and 2000, respectively. She received the M.S. degree in computer engineering from Wright State University, Dayton, OH, in 2003. She is currently working toward the Ph.D. degree from the Department of Neuroscience, Baylor College of Medicine, Houston, TX.

Her research interests are in the areas of computational and systems neuroscience.

Agustin Gutierrez-Galvez received the B.S. degree in physics and in electrical engineering from the Universitat de Barcelona, Spain, in 1995 and 2000, respectively. He received the Ph.D. degree in computer science from Texas A&M University, College Station, in 2005.

His research interests are computational models of the olfactory system and pattern recognition applied to odor detection with sensor arrays.

Ricardo Gutierrez-Osuna (M'00) received the B.S. degree in electrical engineering from the Polytechnic University of Madrid, Spain, in 1992 and the M.S. and Ph.D. degrees in computer engineering from North Carolina State University, Raleigh, in 1995 and 1998, respectively.

From 1998 to 2002, he was on the Faculty of Wright State University, Dayton, OH. He is currently an Assistant Professor of computer engineering at Texas A&M University, College Station. His research interests include pattern recognition, neuromorphic computation, machine olfaction, and speech-driven facial animation.